Theoret. Appl. Mech., Vol.32, No.4, pp. 319–340, Belgrade 2005

Software development for subsonic aircraft's unsteady longitudinal stability derivatives calculation

Nikola Maričić *

Abstract

Subsonic general configuration aircrafts' unsteady longitudinal aerodynamic stability derivatives can be estimated using finite element methodology based on the Doublet Lattice Method (DLM), the Slender Body Theory (SBT) and the Method of Images (MI). Applying this methodology, software DERIV is developed. The obtained results from DERIV are compared to NASTRAN examples HA21A and HA75H. A good agreement is achieved.

Keywords: unsteady aerodynamics, stability derivatives

1 Introduction

During the 60s, as the computer aerodynamics was just starting to develop, the idea to make use of the lifting surfaces theories for estimation of aerodynamic derivatives was proposed [1]. All the theories assume the linear-small amplitude, sinusoidal motion.

To the present day, especially for aircrafts' flutter clearance a lot of methods are developed for accuracy steady and determination of oscillatory aerodynamic loads. Nowadays these loads of general configuration

*Faculty of Technical Sciences at Kosovska Mitrovica, Serbia and Montenegro, e-mail: maricicn@beotel.yu

are calculated using the vortex and doublet-lattice finite elements methods. The chord wise and span wise load distribution on lifting surfaces and longitudinal (z-vertical and y-lateral) load distribution on bodies can be calculated for configurations that consist of an assemblage of lifting surfaces (with arbitrary plan form and dihedral, with or without control surfaces) and bodies (with variable circular or elliptic cross sections).

Aerodynamic finite element methods are based on matrix equation:

$$\{w\} = [A]\{\Delta Cp\}; \quad \Delta Cp = \frac{p_{lower} - p_{upper}}{\rho U^2/2} \tag{1}$$

In Eq.(1) w is column matrix of downwashes (positive down), $[A]$ is square matrix of aerodynamic influence coefficients, and ΔCp is column matrix of dimensionless lifting surface coefficient. The main flow is defined by density ρ and speed U of free stream. Aerodynamic elements are defined by general configuration geometry in the Cartesian coordinate system. The motion of general configuration is defined by degrees of freedom at aerodynamic grid points. Aerodynamic elements are trapezoidal boxes representing the lifting surfaces, ring slender bodies elements, and ring image elements representing slender body and interference influence.

The DLM is used for interfering lifting surfaces in subsonic flow. As DLM is based on the small-disturbance, linear aerodynamics, all lifting surfaces are assumed to nearly lie parallel to main flow. Each interfering surface is divided into boxes. Boxes are small thick less (flat palate) trapezoidal lifting elements. The boxes are arranged to form strips. Strips lay parallel to free stream and the surface edges. Fold and hinge lines lie on the box boundaries. In order to reduce problem size, symmetry option is used. Unknown pressure ΔCp on each box is represented by a line of pressure doublet at quarter chord of the box. Known downwash w collocation (control) point lies at the mid span of the box three quarter chord. DLM aerodynamic elements are represented on Fig.1.

SBT is used to represent lifting characteristics for isolated bodies. SBT assumes that the flow near body is quasi-steady and two-dimensional. Bodies can have z-vertical, y-lateral or both degrees of freedom. Slender bodies of general configuration are divided slender body elements (axial velocity doublets) as shown on Fig.2. Slender body

elements are used to account aerodynamic loading due to motion of the body.

The subsonic wing-body interference is based on the superposition of singularities and their images described in the method of images (MI). Each slender body is substituted by cylindrical interference body, which circumscribes the slender body. The interference body is divided in interference elements, as shown on Fig.3. The interference element is used to include in calculation influence of the other bodies and lifting surfaces on the body, to which element belongs. Each interference element is substituted by z-vertical and y-lateral modified acceleration potential pressure doublets. The primary wing-body interference is accounted for by a system of images of DLM vortices and a system of doublets within each interference element. There is no influence between two interference elements which belong to the same interference body.

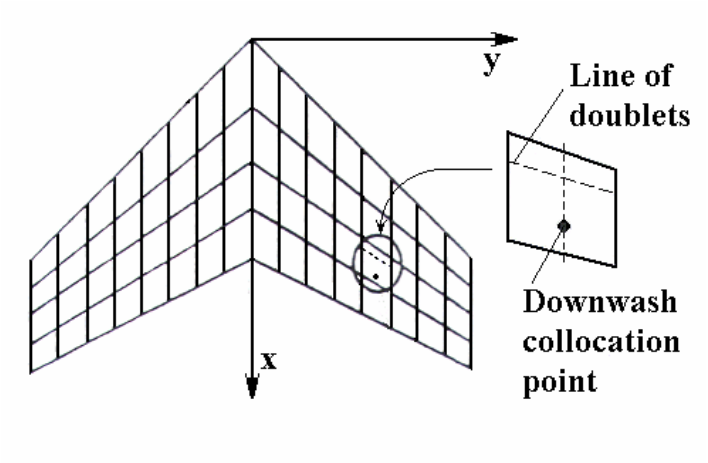

Figure 1:

Based on the above described, matrix Eq.(1) can be written in form:

$$\begin{Bmatrix} \bar{w}_w \\ 0 \\ \bar{w}_s \end{Bmatrix} = \begin{bmatrix} A_{w,w} & A_{w,i} & A_{w,s} \\ A_{i,w} & A_{i,i} & A_{i,s} \\ 0 & 0 & A_{s,s} \end{bmatrix} \begin{Bmatrix} \Delta Cp \\ \mu_i \\ \mu_s \end{Bmatrix}. \qquad (2)$$

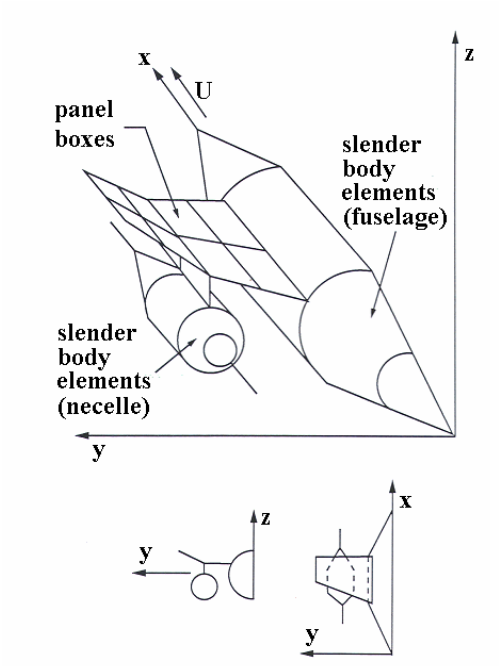

Figure 2:

In Eq.(2):

- $A_{r,s}$ is aerodynamic influence matrix element, which includes part of normal wash of unit strength r-the singularity on s-the finite element. Indexes for the singularities and the aerodynamic finite elements are: w-lifting surface, i-image and s-slender body.
- $\bar{w}_w$ is column of the known downwashes on lifting surface elements in the collocation (control) points normalized by free stream speed U.
- $\bar{w}_i = \{0\}$ is column of zero downwashes on the image elements.
- $\bar{w}_s$ is column of the known downwashes on the slender body elements in axis mid points normalized by free stream speed U.
- ΔCp is unknown column of the strengths of lifting surface singularities (acceleration potential pressure doublets).

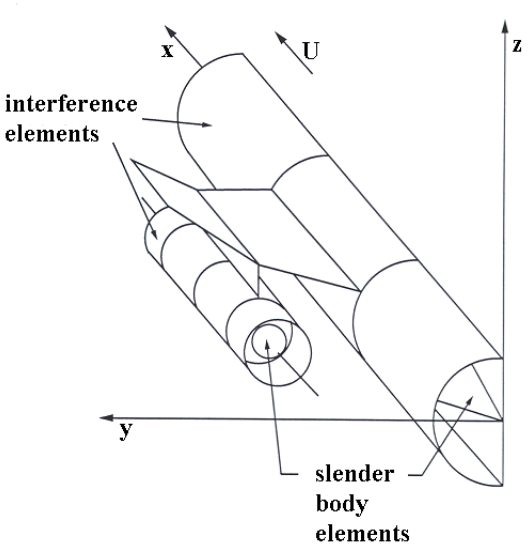

Figure 3:

- μ_i is unknown column of the strengths of images singularities (modified acceleration potential pressure doublets).

- μ_s is known column of the strengths of slender body singularities (velocity potential doublets).

The strength of slender body velocity potential doublet of unit length is known from two-dimensional theory. For j - the slender body element, described by midpoint (ξ, η, ζ) and radius R_j, follows:

$$\mu_{s,j}(\xi, \eta, \zeta, \omega) = 2\pi R_j^2 U \bar{w}_{s,j}(\xi, \eta, \zeta, \omega).$$

In the above relation ω is the angular frequency of the harmonically motion of slender body. As each slender body has z-vertical, y-lateral or both degrees of freedom, generally each j - the element of the body is substituted by the two velocity potential doublets, acting on the real element's axial length $\Delta\xi_j$:

$$\mu_{s,j}^{(y)} = 2\pi R_j^2 U \bar{w}_{s,j}^{(y)} \quad \Delta\xi_j \quad ; \quad \mu_{s,j}^{(z)} = 2\pi R_j^2 U \bar{w}_{s,j}^{(z)} \Delta\xi_j. \tag{3}$$

If boundary values on slender bodies are known, using Eq.(3) the strength of the slender bodies' singularities can be calculated. Substituting these obtained strengths in Eq.(2), it follows:

$$\left\{ \begin{array}{l} \bar{w}_w - \Delta\bar{w}_w \\ -\Delta\bar{w}_i \end{array} \right\} = \left[\begin{array}{ll} A_{w,w} & A_{w,i} \\ A_{i,w} & A_{i,i} \end{array} \right] \left\{ \begin{array}{l} \Delta Cp \\ \mu_i \end{array} \right\}. \tag{4}$$

Here $\bar{w}_w - \Delta\bar{w}_w$ and $-\Delta\bar{w}_i$ are modification of normalized down washes on lifting surface elements and images caused by the known slender body singularities. Eq.(4) represents a system of linear equations with complex coefficients. The system can be solved in terms of the known boundary conditions for the unknowns ΔCp, $\mu_i^{(y)}$ and $\mu_i^{(z)}$.

Lifting surface pressure distribution ΔCp can be integrated to give the lifting surface contributions to the aerodynamic parameters of interest (aerodynamic coefficients, generalized forces, etc.).

The forces on the bodies are determined in more complicated manner. Every lifting surface box ΔCp, every image $\mu_i^{(y)}$ and $\mu_i^{(z)}$, every slender body axis doublet $\mu_s^{(y)}$ and $\mu_s^{(z)}$ affects the force distribution on bodies. It is known from unsteady computational aerodynamics that every singularity can be obtained from the point pressure doublet whose normal wash flow field is obtained from the standard lifting surfaces kernel K. Pressure coefficient $Cp(x, y, z)$ at point (x, y, z) on the body surface due to point pressure doublet of the strength $\Delta Cp(\xi, \eta, \zeta)\Delta A$ in point (ξ, η, ζ) can be obtained by relation:

$$Cp(x, y, z) = \frac{\Delta Cp(\xi, \eta, \zeta)\Delta A}{4\pi} \quad e^{\iota\lambda Ma(x-\xi)} \left(\frac{e^{-\iota\lambda R}}{R} \right). \tag{5}$$

In the above equation:

- Ma is free stream Mach number,
- $R^2 = (x - \xi)^2 + (1 - Ma^2)\left[(y - \eta)^2 + (z - \zeta)^2\right]$,
- $\lambda = \frac{\omega Ma}{U(1-Ma^2)}$ and
- $\vec{N}$ is unit vector in the direction of the doublet.

The term $\Delta Cp(\xi, \eta, \zeta)\Delta A$ is the total pressure doublet strength of lifting surface box of area ΔA in which lifting pressure coefficient is $\Delta Cp(\xi, \eta, \zeta)$.

An equivalent point pressure doublet is assumed to act in $\frac{1}{4}$-mid chord box's point of lifting surface element. The finite length of body doublet $\Delta\xi$ is obtained by two point pressure doublets per each body element. The first is located at the leading edge of the element and has the strength $\mu e^{\frac{\iota\omega\Delta\xi}{2U}}$, and the second at the trailing edge of the strength $-\mu e^{-\frac{\iota\omega\Delta\xi}{2U}}$.

Equation (5) must be integrated over the whole body surface to obtain forces acting on the body due to point doublet located at (ξ, η, ζ). The effects of all point pressure doublets then must be summed to obtain total forces on the body. The detail integration of body force is given in [2].

The main reason for the above described numerical development was the need for accuracy software for aircrafts' flutter clearance. For, in advance, known normal modes of the aircraft's structure the unsteady load distributions on general configuration can be calculated. This possibility can be used to calculate (estimate) steady and unsteady stability aircraft's aerodynamic derivatives. In this case, input data are a few of special rigid body motions of aircraft structure. Definitions of these rigid body motions depend on the case if one needs longitudinal or lateral aircraft's aerodynamic derivatives. In this paper, longitudinal derivatives are analyzed.

Based on the above short description of the used singularities, software package UNAD was developed, used for calculation of unsteady aerodynamic forces of general configuration for flutter calculation. Named package has been modified and package DERIV is developed for steady and unsteady longitudinal aerodynamic derivative calculation of general configuration. Developed software DERIV is tested on NASTRAN examples HA21A and HA75H.

According to the author‘s knowledge in S&CG, projecting teams are using semiempirical method based on NASA's DATCOM software for estimation of unsteady aerodynamic derivatives of general configuration. Software DERIV is the first domestic package that can give steady and unsteady derivatives based on the integration of unsteady aerodynamic loads over the whole aicraft's configuration.

2 Short theoretical outlook

Generally, aircraft's lift and pitch moment coefficients can be represented by the MacLaurent series:

$$C_z = C_{z0} + C_{z\alpha}\alpha + C_{z\dot{\alpha}}\frac{\dot{\alpha}l}{2U} + C_{zq}\frac{\dot{\theta}l}{2U} + C_{z\ddot{\alpha}}\frac{\ddot{\alpha}l^2}{4U^2} + C_{z\dot{q}}\frac{\ddot{\theta}l^2}{4U^2} + \sum_{all\ controls}(C_{z\delta}\delta + C_{z\dot{\delta}}\frac{\dot{\delta}l}{2U} + \cdots) + \cdots, \quad (6)$$

$$C_m = C_{m0} + C_{m\alpha}\alpha + C_{m\dot{\alpha}}\frac{\dot{\alpha}l}{2U} + C_{mq}\frac{\dot{\theta}l}{2U} + C_{m\ddot{\alpha}}\frac{\ddot{\alpha}l^2}{4U^2} + C_{m\dot{q}}\frac{\ddot{\theta}l^2}{4U^2} + \sum_{all\ controls}(C_{m\delta}\delta + C_{m\dot{\delta}}\frac{\dot{\delta}l}{2U} + \cdots) + \cdots \quad (7)$$

In the above two relations, (6) and (7), α is aircraft's angle of attack, q is aircraft's pitch velocity ($q = \dot{\theta}$), where θ is pitch angle over aircrat'c center of gravity (cg) and l is reference length, usually mean wing aerodynamic chord l_{mac}. The total reference angle of atack α_m can be obtained as a linear combination of all involved kinematic effects:

$$\alpha_m = \alpha_{m_0} + \alpha_{m_\alpha}\alpha + \sum_{all\ controls}\alpha_{m_\delta}\delta + \alpha_{m_q}\frac{ql}{2U} + \alpha_{m_{\dot{\alpha}}}\frac{\dot{\alpha}l}{2U} + \sum_{all\ controls}\alpha_{m_{\dot{\delta}}}\frac{\dot{\delta}l}{2U} + \alpha_{m_{\ddot{\alpha}}}\frac{\ddot{\alpha}l^2}{4U^2} + \alpha_{m_{\ddot{\theta}}}\frac{\ddot{\theta}l^2}{4U^2} + \cdots$$

Based on relations (6) and (7), in aircrafts' control theory, steady and unsteady longitudinal aerodynamic derivatives are:

- C_{z0}, C_{m0}, $C_{z\alpha}$, $C_{m\alpha}$, C_{zq}, C_{mq},
- $C_{z\dot{\alpha}}$, $C_{m\dot{\alpha}}$, $C_{z\dot{q}}$, $C_{m\dot{q}}$, $C_{z\ddot{\alpha}}$, $C_{m\ddot{\alpha}}$.

In the Equations (6) and (7), the influences of slats deflections δ_{slat}, flaps deflections δ_{flap}, symmetrical ailerons' deflections δ_{ail}^{symm}, elevaters' deflections δ_{elev} and symmetrical rudders' deflections δ_{rudd}^{symm} (if fins are

positioned out of aircraft's symmetry plane) can be incorporated especially for calculation of the steady longitudinal derivatives. It should be mentioned that the aerodynamic forces on control surfaces strongly depend on their boundary layers. As in the used methods viscosity effects are neglected, derivatives with respect to δ and $\dot{\delta}$ will give only trends to accurate values.

The coefficients C_{z0} and C_{m0} are steady longitudinal derivatives for zero angle of attack ($\alpha = 0$). Values of these derivatives are dominantly influenced by viscosity effects. That's why these derivatives are usually determined on wind tunnel tests. One can use semi-empirical methods or CFD programs (for $\alpha = 0$) to evaluate C_{z0} and C_{m0}, but obtained results are not reliable in many cases. Lucky, for classical general configurations derivatives C_{z0} and C_{m0} are small relative to the other parts in (6) and (7), so their influence can be neglected.

The named aerodynamic longitudinal derivatives may be divided in two groups. One group, in principle, can be obtained by steady methods, while the second one only can be calculated by unsteady methods. When making this distinction, it should be mentioned that,in principle, all derivatives should be computed with an unsteady method.

Generally speaking, aerodynamic stability derivatives are determined in $X_sY_sZ_s$ stability axis system, while aerodynamic forces and moments are calculated aerodynamic axis system $X_aY_aZ_a$. The aerodynamic system is colinear with velocity coordinate system $X_vY_vZ_v$. The axis of aerodynamic system are opposite to the axis of velocity system ($x_a = -x_v$; $y_a = -y_v$; $z_a = -z_v$), when the motion of aircraft is in a straight line. All of the three systems have the same origin in the center of gravity C_{cg} of aircraft structure. The stability and the velocity systems are represented on Fig.4. In connection with relation (6), it is necessary to outline that $C_{z_s} = C_{z_v} = -C_{z_a}$.

In the reference condition the X_a - axis is parallel to airspeed U, but departs from it, X_s - axis is moving with the airplane during a disturbance. That means that the angle of attack α_s, defined as the angle between the X_s - axis and the direction of U, is not necessarily identical to absolute value of the angle of attack $\alpha_a = \alpha$, used in aerodynamic calculations. The axe X_a is in direction of the undisturbed flight path, while X_s - axe is oscillating with rigid airplane. Clearly, α_s represents the disturbance from an aerodynamic state α. As small disturbances

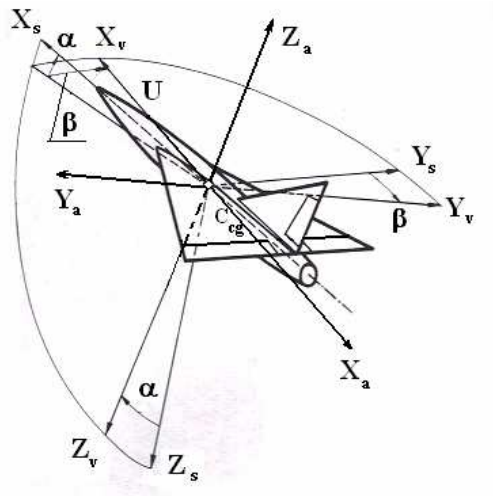

Figure 4:

have been assumed, simple conversion rules between the stability and the aerodynamic axis systems for symmetric motions are:

$$X_sY_sZ_s \Rightarrow -\alpha = \iota k\frac{h_z}{l_{mac}} + \theta \Leftarrow X_aY_aZ_a,$$

$$X_sY_sZ_s \Rightarrow -q = \iota k\theta \Leftarrow X_aY_aZ_a.$$

In the stability axis system α_s - variation is equivalent to a variation of down wash of the airplane. So, it is equivalent to the angle of attack to be prescribed in the methods used in this paper, where the aerodynamic axis system is used. A q-variation, as defined in the stability axis system, is felt by the airplane as linearly varying down wash in the aerodynamic system

As already stated in the introduction of this paper, concept of integration of unsteady aerodynamic loads is used, so that obtained lift $\bar{C}_z$ and pitch moment $\bar{C}_m$ coefficients are complex numbers. These complex coefficients are connected to (6) and (7) by relations:

$$C_z = \Re e(\bar{C}_z e^{\iota\omega t}); \quad C_m = \Re e(\bar{C}_m e^{\iota\omega t}). \tag{8}$$

In order to calculate unsteady longitudinal derivatives, three general configuration motions are of interest. The first is quasi-steady harmonic

change of attack angle, the second is slow steady pitch and the third is aircraft's quasi-steady harmonic vertical translation:

A1 Quasi-steady harmonic change of the angle of attack $\Rightarrow \alpha(x,y,z,t)$; $\alpha_0 = const.$

$$\alpha = \alpha_0 e^{\iota\omega t} \;\Rightarrow\; \dot{\alpha} = \iota\omega\alpha \;\Rightarrow\; \ddot{\alpha} = -\omega^2\alpha. \tag{9}$$

A2 Slow steady pitch angle $\Rightarrow$ $\theta(x,y,z,t)$; $q = \frac{d\theta}{dt} = const.$

By introducing a constant pitch angular velocity q, it follows that

$$\theta = \frac{q(x-x_{cg})}{U} = \frac{ql_{mac}}{2U}\frac{2(x-x_{cg})}{l_{mac}} \equiv \frac{\partial h_{0p}}{\partial x}. \tag{10}$$

For the value $\frac{ql_{mac}}{2U} = 0.1$ Eq. (11) can be integrated:

$$\frac{dh_{0p}}{dx} = \frac{.2(x-x_{cg})}{l_{mac}} \quad \Leftrightarrow \quad h_{0p} = 0.1\frac{(x-x_{cg})^2}{l_{mac}}. \tag{11}$$

It is clear that, $dh_{0p}/dt = 0$.

A3 Quasi-steady harmonic vertical translation $\Rightarrow h_z(t)$; $dh_z/dx = 0$

$$\begin{aligned} h_z &= h_{0z}e^{\iota\omega t} \;\Rightarrow\; \dot{h}_z = \iota\omega h_z \equiv \alpha_z U \;\Rightarrow \\ \alpha_z &= \iota\frac{\omega}{U}h_z = \iota\frac{k}{l_{mac}}h_z; \\ k &= \frac{\omega l_{mac}}{U} \end{aligned} \tag{12}$$

Angle α_z is the angle of attack (from stability axis system) induced by small amplitude quasi-steady harmonic vertical oscillations h_z relative to the path of aircraft motion. In relation (12) k is reduced frequency.

As in the steady calculations harmonic vertical translation doesn't exist and vs. in the unsteady calculations slow steady pitch doesn't exist, the cases A2. and A3. can be treated as one case.

In the flutter calculation the boundary conditions can be obtained from aircraft's structure normal modes' shapes (deflections and slopes of mode shape). In, per example [7], is shown that the boundary condition – normalized downwash on each lifting surface or body's element is:

$$\begin{aligned} \bar{w}_{i_j} &= \frac{w_{i_j}}{U} = \frac{dh_{0_j}}{dx} + \frac{1}{U}\frac{dh_{0_j}}{dt} = \frac{dh_{0j}}{dx} + \iota\frac{\omega}{U}h_{0_j}; \\ h_i(x_j, y_j, z_j, t) &= \Re e[h_{0_i}(x_j, y_j, z_j)e^{\iota\omega t}] \end{aligned} \tag{13}$$

In Eq. (13), the index j is the number of element and the index i is the normal mode number.

Using the same idea, in order to calculate the previously mentioned longitudinal derivatives, seven harmonic rigid body (quasy-steady o steady) motions of the general configuration, instead of normal modes, have to be incorporated:

B1 Quasi-steady harmonic change of the angle of attack In developed software $\alpha_0 = 0.1$ is default value, as it is acceptable in the used linear theories.

- On lifting surface $j - the$ element in point (x, y, z)

$$\begin{aligned} h_{0_1}(x, y, z) &= tg\alpha_0(x_{cg} - x)\cos\gamma_j; \\ \frac{\partial h_{0_1}}{\partial x} &= -tg\alpha_0\cos\gamma_j \end{aligned} \tag{14}$$

  Variable γ_j is dihedral angle of $j - the$ lifting surface element.

- On image body axe $j - the$ element in midpoint (x, y, z) in vertical direction

$$h_{0_1}(x, y, z) = tg\alpha_0(x_{cg} - x); \quad \frac{\partial h_{0_1}}{\partial x} = -tg\alpha_0 \tag{15}$$

B2 Steady pitch and quasi-steady harmonic vertical translation

In developed software $\frac{ql_{mac}}{2U} = 0.1$ and $\bar{h}_z = 0.1\frac{l_{mac}}{2}$ are default values, as they are acceptable in the used linear theories.

- For steady pitch on lifting surface $j-the$ element in point (x,y,z) it follows

$$\begin{aligned} h_{0_2}(x,y,z) &= - 0.1\frac{(x-x_{cg})^2}{l_{mac}}\cos\gamma_j; \\ \frac{\partial h_{0_2}}{\partial x} &= - 0.2\frac{x-x_{cg}}{l_{mac}}\cos\gamma_j \end{aligned} \tag{16}$$

On lifting surface $j-the$ element in point (x,y,z) in quasi-steady hamonic vertical translation

$$h_{0_2}(x,y,z) = -\bar{h}_z \quad \cos\gamma_j; \quad \frac{\partial h_{0_2}}{\partial x} = 0 \tag{17}$$

- On image body axe $j-the$ element in midpoint (x,y,z) in vertical direction for steady pitch, it follows:

$$\begin{aligned} h_{0_1}(x,y,z) &= - 0.1\frac{(x-x_{cg})^2}{l_{mac}}; \\ \frac{\partial h_{0_1}}{\partial x} &= - 0.2\frac{x-x_{cg}}{l_{mac}} \end{aligned} \tag{18}$$

On image body axe $j-the$ element in point (x,y,z) in quasi-steady harmonic vertical translation in vertical direction

$$h_{0_2}(x,y,z) = -\bar{h}_z; \quad \frac{\partial h_{0_2}}{\partial x} = 0 \tag{19}$$

B3 Steady slats' deflection

The default slat deflection is $\delta_{slat} = 0.1$. Only lifting surface elements on the wing's slats are deflected. In any slat control point (x_{kj}, y_{kj}, z_{kj}) it follows:

$$h_{0_3} = \delta_{slat}(x_{kj} - x^{arm}_{k,slot})\cos\lambda_{slat} \quad ; \quad \frac{\partial h_{0_3}}{\partial x} = \delta_{slat}\cos\lambda_{slat} \tag{20}$$

In the above relations, $x^{arm}_{k,slot}$ is distance from control point to slat rotation axe and λ_{slat} is the swept angle of slat rotation axe. On all the other elements, meaning on all the other lifting surface elements and image bodies elements $h_{0_3} = 0$ and $\frac{\partial h_{0_3}}{\partial x} = 0$.

B4 Steady flaps' deflection

The default flap deflection is $\delta^{=}_{flap} 0.1$. Only lifting surface elements on the wing's flaps are deflected. In any flap control point (x_{kj}, y_{kj}, z_{kj}) it follows:

$$h_{0_4} = \delta_{flap}(x_{kj} - x^{arm}_{k,flap}) \cos\lambda_{flap}; \quad \frac{\partial h_{0_4}}{\partial x} = \delta_{flap} \cos\lambda_{flap} \qquad (21)$$

In Eq. (21), $x^{arm}_{k,flap}$ is distance from control point to flap rotation axe and λ_{flap} is the swept angle of flap rotation axe. On all other elements, meaning on all the other lifting surface elements and image bodies elements $h_{0_4} = 0$ and $\frac{\partial h_{0_4}}{\partial x} = 0$.

B5 Steady symmetric ailerons' deflection

If ailerons have different up and down deflection angles, any combination of their deflections can be obtained as sum of symmetrical and anti symmetrical deflections.

$$\delta^{symm}_{ail} = \frac{1}{2}(\delta^{down}_{ail} + \delta^{up}_{ail}); \quad \delta^{anti}_{ail} = \frac{1}{2}(\delta^{down}_{ail} - \delta^{up}_{ail})$$

The default symmetric aileron deflection is $\delta^{symm}_{ail} = 0.1$. Only lifting surface elements on the wing's ailerons are deflected. In any aileron control point (x_{kj}, y_{kj}, z_{kj}) it follows:

$$h_{0_5} = \delta^{symm}_{ail}(x_{kj} - x^{arm}_{k,ail}) \cos\lambda_{ail}; \quad \frac{\partial h_{0_5}}{\partial x} = \delta^{symm}_{ail} \cos\lambda_{ail} \qquad (22)$$

In the above relations, $x^{arm}_{k,ail}$ is distance from control point to aileron rotation axe and λ_{ail} is the swept angle of aileron rotation axe. On all the other elements, meaning on all the other lifting surface elements and image bodies elements $h_{0_5} = 0$ and $\frac{\partial h_{0_5}}{\partial x} = 0$.

B6 Steady elevators' deflection

The default symmetric elevator deflection is $\delta_{elev} = 0.1$. Only lifting surface elements on the tail's elevator are deflected. In any elevator control point (x_{kj}, y_{kj}, z_{kj}) it follows:

$$h_{0_6} = \delta_{elev}(x_{kj} - x^{arm}_{k,elev}) \cos\lambda_{elev}; \quad \frac{\partial h_{0_6}}{\partial x} = \delta_{elev} \cos\lambda_{elev} \tag{23}$$

In Eq. (23), $x^{arm}_{k,elev}$ is distance from control point to elevator rotation axe and λ_{elev} is the swept angle of elevator rotational axe. On all the other elements, meaning on all the other lifting surface elements and image bodies elements $h_{0_6} = 0$ and $\frac{\partial h_{0_6}}{\partial x} = 0$.

B7 Steady symmetric rudders' deflection

If aircraft's fin is out of symmetry plane than steady aerodynamic derivatives for rudder symmetric deflection can be obtained. Usually in this case general configuration incorporates two fins out of aircraft's symmetry plane. The default symmetric rudder deflection is $\delta^{symm}_{rudd} = 0.1$. Only lifting surface elements on the fins' rudders are deflected. In any rudder control point (x_{kj}, y_{kj}, z_{kj}) it follows:

$$\begin{aligned} h_{0_7} &= \delta^{symm}_{rudd}(x_{kj} - x^{arm}_{k,rudd}) \cos\delta_{rudd}; \\ \frac{\partial h_{0_7}}{\partial x} &= \delta^{symm}_{rudd} \cos\lambda_{rudd} \end{aligned} \tag{24}$$

In the above relations, $x^{arm}_{k,rudd}$ is distance from control point to rudder rotation axe and λ_{rudd} is the swept angle of rudder rotation axe. On all the other elements, meaning on all the other lifting surface elements and image bodies elements $h_{0_7} = 0$ and $\frac{\partial h_{0_7}}{\partial x} = 0$.

Substituting (9) and (10) into (8) one can obtain:

$$\begin{aligned} \bar{C}_z &= \alpha_0[C_{z\alpha} + \iota k(C_{z\dot{\alpha}} + C_{zq})]; \\ \bar{C}_m &= \alpha_0[C_{m\alpha} + \iota k(C_{m\dot{\alpha}} + C_{mq})] \end{aligned} \tag{25}$$

Taking $\Im m(\bar{C}_z)$ and $\Im m(\bar{C}_m)$ from relations (25) it follows:

$$C_{z\dot{\alpha}} = \frac{1}{k}\Im m\frac{\bar{C}_z}{\alpha_0} - C_{zq}; \quad C_{m\dot{\alpha}} = \frac{1}{k}\Im m\frac{\bar{C}_m}{\alpha_0} - C_{mq} \tag{26}$$

Steady longitudinal derivatives $C_{z\alpha}$, $C_{m\alpha}$, C_{zq} and C_{mq}can be determined from integration of all over general configuration aerodynamic loadings in steady flow condition for steady boundary conditions ($k = 0$) by introducing (9) and (10) into (13).

In order to account unsteady longitudinal derivatives $C_{z\ddot{\alpha}}$ and $C_{m\ddot{\alpha}}$, it is necessary to introduce (11) into (8). Then one can obtain:

$$\begin{aligned} \frac{\bar{C}_z}{h_z/l_{mac}} &= \iota k C_{z\alpha} - k^2 C_{z\dot{\alpha}} - \iota k^3 C_{z\ddot{\alpha}}; \\ \frac{\bar{C}_m}{h_z/l_{mac}} &= \iota k C_{m\alpha} - k^2 C_{m\dot{\alpha}} - \iota k^3 C_{m\ddot{\alpha}} \end{aligned} \tag{27}$$

Taking $\Im m(\bar{C}_z^{)}$ and $\Im m(\bar{C}_m)$ from relations (27) it follows:

$$\begin{aligned} C_{z\ddot{\alpha}} &= \frac{1}{k^3}\left[\Im m\left(\frac{\bar{C}_z}{h_z/l_{mac}} + k^2 C_{z\dot{\alpha}}\right) + kC_{z\alpha}\right]; \\ C_{m\ddot{\alpha}} &= \frac{1}{k^3}\left[\Im m\left(\frac{\bar{C}_m}{h_z/l_{mac}} + k^2 C_{m\dot{\alpha}}\right) + kC_{m\alpha}\right]. \end{aligned}$$

For determination of unsteady derivatives, it is necessary to develop (6) and (7) in the MacLaurent series of higher order and it follows:

$$\begin{aligned} \bar{C}_z &= \alpha_0[C_{z\alpha} + \iota k(C_{z\dot{\alpha}} + C_{zq}) - k^2(C_{z\ddot{\alpha}} - C_{z\dot{q}})] \\ \bar{C}_m &= \alpha_0[C_{m\alpha} + \iota k(C_{m\dot{\alpha}} + C_{mq}) - k^2(C_{m\ddot{\alpha}} - C_{m\dot{q}})] \end{aligned} \tag{28}$$

In (28) only $C_{z\dot{q}}$ and $C_{m\dot{q}}$ are unknowns. So, taking $\Re e(\bar{C}_z)$ and $\Re e(\bar{C}_m)$ from (28) one can find:

$$\begin{aligned} C_{z\dot{q}} &= -C_{z\ddot{\alpha}} - \frac{1}{k^2}\left\{C_{z\alpha} - \Re e\left[\frac{\bar{C}_z}{\alpha_0} - \iota k(C_{z\dot{\alpha}} + C_{zq})\right]\right\}, \\ C_{m\ddot{q}} &= -C_{m\ddot{\alpha}} - \frac{1}{k^2}\left\{C_{m\alpha} - \Re e\left[\frac{\bar{C}_m}{\alpha_0} - \iota k(C_{m\dot{\alpha}} + C_{mq})\right]\right\}. \end{aligned} \tag{29}$$

3 Examples

Two examples from the well known software NASTRAN are tested. The first example was case HA21A for steady longitudinal aerodynamic derivatives, and the second was case HA75H for unsteady flow.

3.1 Case HA21A

The case is taken from [3]. Forward-Swept-Wing (FSW) airplane with coplanar canard-wing configuration was tested in trimmed see level steady flight at Mach number 0.9. The model is idealized as shown on Fig.5.

The wing has an aspect ratio of 4.0, no taper, twist, camber, or incidence relative to fuselage, and a forward sweep angle of 30^o. The canard has an aspect ratio of 1.0, and no taper, twist, camber, incidence, or sweep. The chords of both the wing and canard are $3050,00$ [mm], and reference length is equal to the wing mid aerodynamic chord $l_{mac} = 3050,00$[mm]. The half-span model of aircraft is divided on 32 equal panels (8 span-wise, 4 chord-wise) on the wing and 8 equal panels (2 span-wise, 4 chord-wise) on the canard. The fuselage length is $9150,00$ [mm]. Aerodynamic forces on the fuselage are neglected.

The aerodynamic coordinate system is located in the beginning of the fuselage in coplanar plane of wing-canard configuration. Center of gravity is $4575,00$[mm] behind aerodynamic coordinate system origin in mid point of canard root-chord.

The comparison of results from [3] and DERIV are given in Table 1. Steady derivatives $C_{z\delta_c}$ and $C_{m\delta_c}$ are related to canard deflection δ_c.

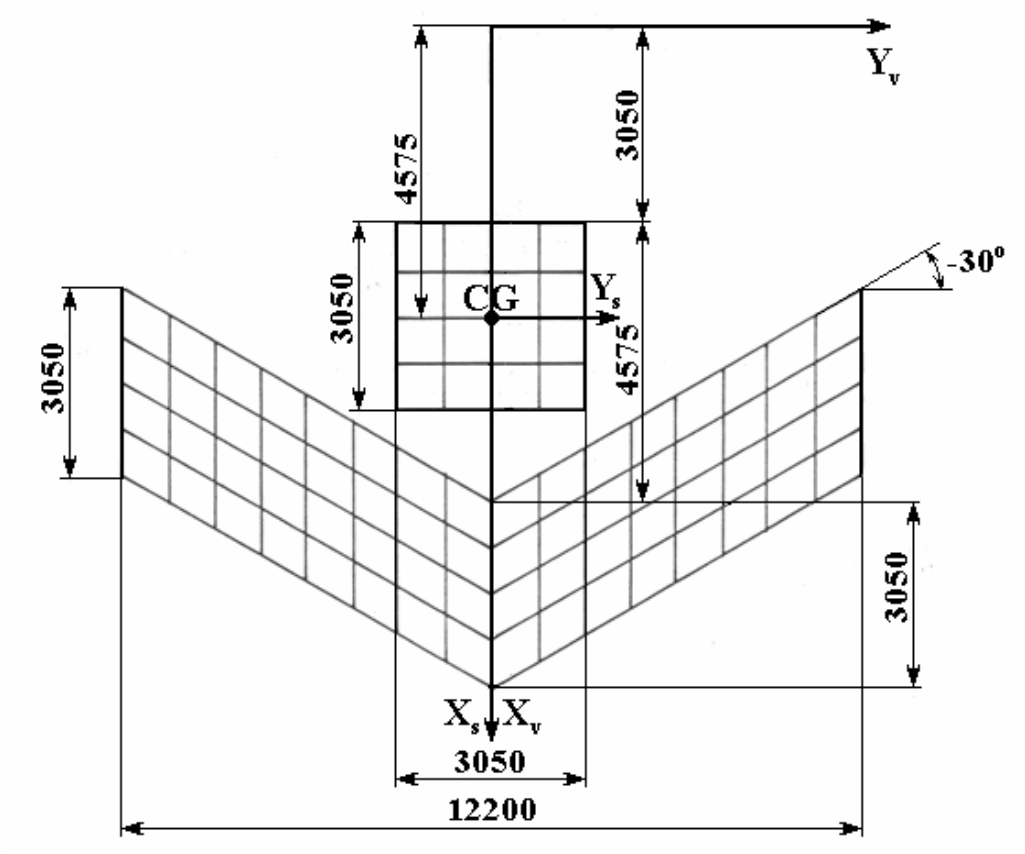

Figure 5:

Software	$C_{z\alpha}$	$C_{m\alpha}$	C_{zq}	C_{mq}	$C_{z\delta_c}$	$C_{m\delta_c}$
NASTRAN[3]	-5.0711	-2.8712	-12.0746	-9.9549	-0.2461	0.5715
DERIV	-5.0710	-2.8710	-12.0740	-9.9540	-0.2461	0.5715

Table 1:

Based on the results given in Table 1. steady longitudinal aerodynamic derivatives from NASTRAN and DERIV are in good agreement.

3.2 Case HA75H

The case is taken from [5] and [6]. Typical transport aircraft's wing was tested in unsteady flow at Mach number 0.8 at see level. Geometry of the wing is given on Fig.6. The wing has an aspect ratio of 8.0, taper $l_{tip}/l_{root} = 0.25$, no twist, camber, or incidence relative to fuselage, and a leading edge sweep angle of 33.1142^o. The sweep angle of the wing mean aerodynamic chords' line is 30^o. The pitch axe of the wing includes point at $l_{mac}/4$. In the wing's symmetry plane origin of pitch axe is at 827.35[mm] behind leading edge of the wing's root chord. The half-span model of wing is divided in 75 panels (15 equal span-wise, 5 equal chord-wise).

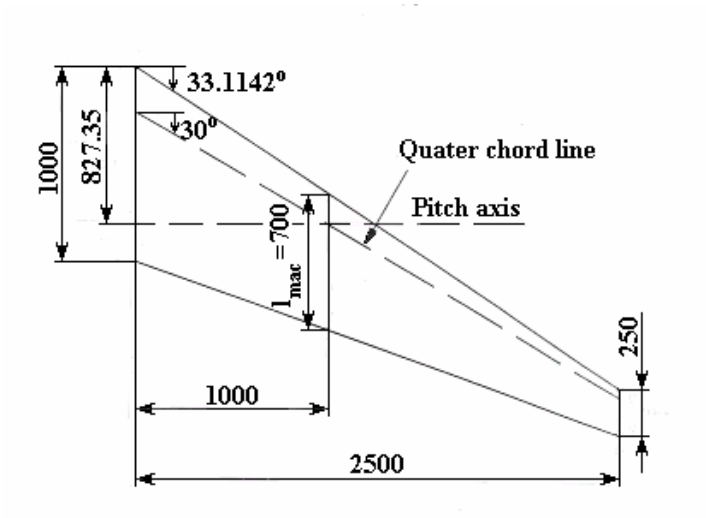

Figure 6:

In [6] and DERIV moments' derivatives are calculating for pitch axe located in wing symmetry's plane at $l_{mac}/4$. As in [5] pitch axe was in leading wing edge in its symmetry plane, it was necessary to recalculate moments' derivatives. If $(C_{m*})_1$ and $(C_{m*})_2$ are moments' derivatives

for longitudinal location of pitch axe x_1 andx_2, respectively, then they are correlated using relation:

$$(C_{m*})_2 = (C_{m*})_1 \quad + C_{z*}\frac{x_1 - x_2}{l_{mac}}$$

In the Table 2. calculated steady and unsteady longitudinal aerodynamic derivatives are given, taken from [5], [6] and DERIV. Unsteady derivatives are compared for reduced frequency $k = \omega l_{mac}/(2U) = 0.010$. The data marked as (*) in the Table 2. are not represented in [5] or [6].

	[5]	[6]	DERIV
$C_{m\alpha}$	(*)	- 5.8490	- 5.8455
$C_{m\alpha}$	(*)	- 0.5643	- 0.5847
C_{zq}	(*)	- 5.9360	- 5.9978
C_{mq}	(*)	- 3.2050	- 3.2887
$C_{z\dot{\alpha}}$	12.5300	12.5400	12.4325
$C_{m\dot{\alpha}}$	0.8504	0.8744	0.8980
$C_{m\dot{q}}$	-16.4000	(*)	-16.3317
$C_{m\dot{q}}$	(*)	(*)	0.7749
$C_{z\ddot{\alpha}}$	94.7000	(*)	93.7748
$C_{m\ddot{\alpha}}$	11.6375	(*)	11.1347

Table 2:

Based on the Table 2., the results for HA75H obtained from [5], [6] and DERIV are in good agreement.

4 Conclusion

Shortly described, the developed methodology and test results of developed software DERIV for calculation of unsteady longitudinal aerodynamic derivatives for general configurations are given in the paper.

The obtained results from developed software DERIV are in good agreement to results from NASTRAN.

References

[1] B.Etkin: Dynamics of flight, Wiley, New York, 1959.

[2] J.Giesing, T.Kalman, W. Rodden: Subsonic Unsteady Aerodynamics for General Configurations, Part II, Vol. I, Wright-Patterson Air Force Dynamic Laboratory, Tech.Rep. AFFDL-TR-71-5, Ohaio, April 1972.

[3] E.Bellinger: MSC/NASTRAN Aeroelastic Supplement, The MacNeal Schwendler Corporation, Los Angeles, June 1986.

[4] N.Maricic: Contribution to calculation of aircraft's critical flutter speeds, Ph.D.dissertation, Faculty of Mechanical engineering, Belgrade, January 1990. (in Serbian)

[5] W.Rodden, J.Geising: Application of Oscillatory Aerodynamic Theory of Estimation of Dynamic Stability Derivatives, J.Aircraft, Vol.21, No. 1, January, 1984.

[6] W.Rodden, E.Bellinger, J.Geising: Errata and Addenda to "Application of Oscillatory Aerodynamic Theory of Estimation of Dynamic Stability Derivatives, J.Aircraft, Vol.21, No. 1, January, 1984.

[7] T.Dragovic: Unsteady Aerodynamics, Mimeographed notes for Higher Military Aeronautical Technical Academy, Belgrade, 1976. (in Serbian)

Submitted on June 2005, revised on December 2005.

Razvoj softvera za proračun nestacionarnih, uzdužnih aerodinamičkih derivativa podzvučnih aviona

UDK 536.7

Nestacionarni, uzdužni aerodinamički derivativi subsoničnih aviona proizvoljne konfiguracije mogu se proceniti korišćenjem metoda konačnih elemenata baziranih na metodi rešetke dubleta (Doublet Lattice Method – DLM), teoriji vitkih tela (Slender Body Theory – SBT) i metodi zamena (Method of Images – MI). Primenom navedene metodologije razvijen je softverski paket DERIV. Rezultati dobijeni programom DERIV testirani su na primerima HA21A i HA75H iz NASTRAN-a. Postignuto je dobro slaganje rezultata.